Research papers

The Rivillas flood of 5–6 November 1997 (Badajoz, Spain) revisited: An approach based on *Iber+* modelling

José González-Cao [a,*], Diego Fernández-Nóvoa [a,b], Orlando García-Feal [a], Jose R. Figueira [c], José M. Vaquero [d], Ricardo M. Trigo [b], Moncho Gómez-Gesteira [a]

[a] *Environmental Physics Laboratory (EPhysLab), CIM-UVIGO, Universidade de Vigo, Campus As Lagoas s/n, 32004 Ourense, Spain*
[b] *Instituto Dom Luiz (IDL), Faculdade de Ciências da Universidade de Lisboa, 1749-016 Lisbon, Portugal*
[c] *Departamento de Expresión Gráfica, Universidad de Extremadura, Mérida, Spain*
[d] *Departamento de Física, Universidad de Extremadura, Mérida, Spain*

A B S T R A C T

The flash flood registered in November 1997 in the city of Badajoz (Spain) in the basin of Rivillas river is analysed by means of the numerical code *Iber+*. This event constitutes one of the most destructive flash-floods registered in an urban area in the Iberian Peninsula. Starting from precipitation data obtained from rain stations, the runoff of the entire river basin was simulated to obtain the discharge of the Rivillas river in Badajoz. The flood maps obtained with *Iber+* reproduce accurately the field data registered during the actual event. Likewise, the numerical time evolution of the flood and water depths are in accordance with testimonies of the witnesses. Once the capability of *Iber+* to reproduce the event was assessed, several scenarios were considered in order to analyse the main causes of the event. In particular, simulations show that the catastrophic magnitude of the flood was mainly due to the blockage of bridges. Different hypothetical scenarios were simulated to analyze the role of rain intensity and bridge maintenance, concluding that similar floods can occur under much lower rainfall but with poor bridge maintenance.

1. Introduction

The recent release of the 6th Assessment Report by the International Panel of Climate Change (IPCC, 2021) confirms that humans are already having a very significant impact in many branches of the climate system and that this will increase in the coming decades, independently of the climate scenarios considered. The effects of Climate Change are widespread including a number of changes in the hydrological cycle, namely in terms of the increment of extreme precipitation events both in frequency and intensity (Groisman et al., 2005; Beniston, 2009; Morss et al., 2011). It is within this context that most experts have framed the recent flood events registered in July 2021 in China and Central Europe (Germany and Belgium) that caused more than 500 deceases and billions of euros in economic loses (EFAS, 2021). Therefore, the capability to predict well in advance these events is a crucial task in order to minimise their future negative effects. One of the main approaches to deal with this problem is through numerical simulations. In recent years, the development of numerical tools, strongly sustained on the increment of the computational power, has facilitated the ability of the numerical

simulations to reproduce such events with increasing detail. These simulations allow a far better understanding of the effect of Climate Change related with flood events and can contribute with relevant information to mitigate their downsides. According to the European directive (E.D. 2007/60/C), it is important to assess potential risks derived from flood events through: *"a description of the floods which have occurred in the past and which have had significant adverse impacts on human health, the environment, cultural heritage and economic activity and for which the likelihood of similar future events is still relevant, including their flood extent and conveyance routes and an assessment of the adverse impacts they have entailed"*, which highlights the importance of reproducing past extreme flood events with numerical tools.

Literature shows many examples of past flash-floods derived from extreme precipitation events. Vennari et al. (2016) provide a database of about 500 flash-flood events registered in small catchments located in Campania (Southern Italy) from 1540 to 2015. Zêzere et al. (2020) provide a comprehensive collection of floods registered in mainland Portugal in the period 1865–2015 located in the Tagus, Douro, Mondego, and Vouga valleys. Trigo et al. (2016) analyse the main causes

behind one of the deadliest flash-floods occurred in Portugal, which took place on the 25 and 26 November 1967.

Following a historical perspective, Eulenstein and Kellerer-Pirklbauer (2020) provide a detailed description of the flood event registered in central Europe (catchments of Danube and Vltava) in 1572 using geographical sources. Bárdossy et al. (2020) analyse the historical flood event registered in 1882 in Neckar catchment (West Germany) using the fully distributed spatial modelling HBV (Bergström, 1992). Elleder et al. (2020a) describe the catastrophic flood registered in the Bohemian-Moravian Highlands (Sázava River) in 1714 and Elleder et al. (2020b) analyse the consequences of torrential rain event in the city of Prague (Czech Republic) in 1872. Other interesting works focused on past flood events are Buzzi et al. (1998) where the flood registered in 1994 in Piedmont (northwestern Italy) is reproduced or Bartholmes and Todini (2005) where the authors reproduce the extreme event registered in November 1994 in the catchment of the Po river. One of the most important years concerning the number and magnitude of flood events is 1876. The bibliography shows several examples of floods registered all over the world that year. For example, Benito et al. (1996) and Font (1988) describe floods of several rivers in Spain. Other countries were also affected during that year by extreme floods: Portugal (González, 1995; Trigo et al., 2014), France, and Germany (Pfister et al., 1999). Recently, González-Cao et al. (2021) have also applied a multi-modelling approach to the analysis of historical floods in western Iberia. In that work the authors reproduce the flood event registered on 5 December 1876 in Badajoz using the numerical code *Iber+* (García-Feal et al., 2018) and the effects in the city are analysed in detail. The reader can find other interesting works related to historical floods in Máyer Suárez (2002) where a series of flood events registered in Las Palmas (Spain) from 1865 to 1999 are described and in Laguarda (1962) where the flood registered in Valencia in 1957 is shown. More recent events are analysed by Chao et al. (2021). This study analyses flood events registered from May 2013 to September 2014 in the Daheba Watershed (China). Hermoso et al. (2021) analyse the event registered on 12 and 13 September 2019 in several Eastern areas of the Iberian Peninsula.

One of the most destructive flash-floods registered in an urban area in the Iberian Peninsula during 20th Century was registered on the 5th and 6th November 1997 in the city of Badajoz. During the last hours of 5th and the first hours of day 6th, the Rivillas river flooded several areas of the city causing 21 deceases and high economic losses. As it was previously pointed, the capability to reproduce and predict such events by means of numerical tools is a crucial task in order to minimise negative effects in future scenarios. *Iber* is a numerical code widely used in many fields of hydrology. For example, González-Cao et al.(2019) and Fernández-Novoa et al. (2020) developed an early warning system for flood prediction in the Miño river (Northwestern Spain) based on rainfall forecast by coupling the code HEC-HMS to model the runoff processes and *Iber* to obtain hazard maps at several locations. In González-Cao et al. (2020) the authors reproduced the flood derived by the break of Malpasset dam (France) in 1959. Bonasia and Ceragene (2021) carried out an application of *Iber* to define the potential flood points located in the ungauged river basin of La Sabana river (Mexico). Related with past events, Benito et al. (2021) reproduced a series of floods registered in the Duero basin (Spain) from 1250 to 1871. In this work *Iber* allows an accurate estimation of the peak values of discharge associated to these events starting from field data obtained from documentary evidences as minute books, newspapers and water marks. In Bermúdez et al. (2021) *Iber* was applied to analyse past and future flood events registered in coastal river areas analysing the effects of the climate change both in river discharges and in the rising of mean sea level. Similar to these works Ruman et al. (2021) applied *Iber* to estimate the discharge of the flood event registered in December 2000 in Crete (Greece) by using six paleostage indicators to calibrate the model. In addition to the analysis of flood events, the Iber model has been applied to other fields. Thus, Mateo-Lázaro et al. (2020) shows an application of *Iber* to analyse the

impact of structures, as for example bridges, on the current of rivers comparing velocities and water depths before and after the installation of such structures. Aranda et al. (2021) applied *Iber* to design effective drainage systems of transportation facilities. In García-Alén et al. (2021) the authors applied *Iber* to reproduce the water flow in the presence of obstacles as weirs. A dataset of 194 experiments of nine different weir geometries were used to quantify the discrepancies of the numerical results. Finally, to show the wide range of applications of *Iber*, the reader can find an interesting application to the analysis of water quality in García-Feal et al. (2020). In this paper the authors develop the *IberWQ* suite based on *Iber* to compute the most relevant parameters used to evaluate water quality as, for example, dissolved oxygen, organic nitrogen, ammonia, nitrates among others.

The main aim of the present work is both the numerical reproduction of the event registered on the 5th and 6th November 1997 in the city of Badajoz using the *Iber+* numerical code and the analysis its causes through the reproduction of a series of hypothetical flood scenarios in order to prevent and reduce the risk of similar events in the future. The document is organized as follows: in Section 2, the area of study, the evolution of the flood event and its consequences in Badajoz are described. Then, the precipitation dataset along with hydraulic model used are briefly presented in Section 3. The numerical results of discharge flow and the water depths registered during the flood event in Badajoz are shown in Section 4. Moreover, numerical results are also shown, obtained for various hypothetical scenarios derived from the current one. Finally, Section 5 provides the main conclusions of this work.

2. Area of study and description of the event

The whole area of study (Fig. 1) can be divided into two subareas, namely the basin of the Rivillas river before reaching the city of Badajoz, and the urban area where the river is canalized. The basin of the Rivillas river is located in the south-west of the Iberian Peninsula and covers an area of 314 km^2 (Fig. 1a). The Rivillas river has an approximate length of 41 km and, as such, can be considered a small tributary of the Guadiana river. The elevation of Rivillas catchment ranges from 350 m.a.s.l. at the headwater near Valverde de Leganés (see Fig. 1b) to near 174 m.a.s.l. at the mouth, located in Badajoz (Spain). Calamón river is the main tributary of Rivillas river and their junction, located in the urban area of the river (Fig. 1c), is located ∼ 1.5 km upstream from the mouth of Rivillas river. Several bridges are located in the urban area of the domain. Fig. 2 shows the current location of these bridges. Some of them acted as barriers during the event registered in 1997. A detailed description of the Rivillas river is shown in Zamora-Cabanillas (1999) and in Ortega (2007).

Badajoz suffered the most adverse effects derived from the floods registered on the 5th and 6th November 1997. The event corresponds to one of the most extreme precipitation events in the western Iberian Peninsula in 20th Century. Other cities or villages like Mérida or Valverde de Leganés, in Spain, and several areas in Portugal were also affected by this event but the consequences were less dramatic than in Badajoz. Newspapers and testimonies of survivors are the main source of information related to the impact of this extreme precipitation event. Several newspapers in Spain described in detail the evolution and consequences of the flood in the city of Badajoz. They highlight the consequences of the event: 21 deceases and economic losses of $100 M USD. First-hand testimonies from survivors are also a valuable source of information in order to understand the evolution of the flood. Technical reports and other studies (CEDEX, 1998; Zamora-Cabanillas, 1999; Ortega, 2007) have also focused on this extreme flood. All these works show that during the days 5th and 6th the precipitation registered in several rain stations near Badajoz reached historical records. For example, in Talavera La Real the total amount for those two days (from 8 a.m., 5th November to 8p.m., 6th November) was 119 mm, in La Albuera 110 mm and in Pantano de Piedraguda 133 mm. These figures
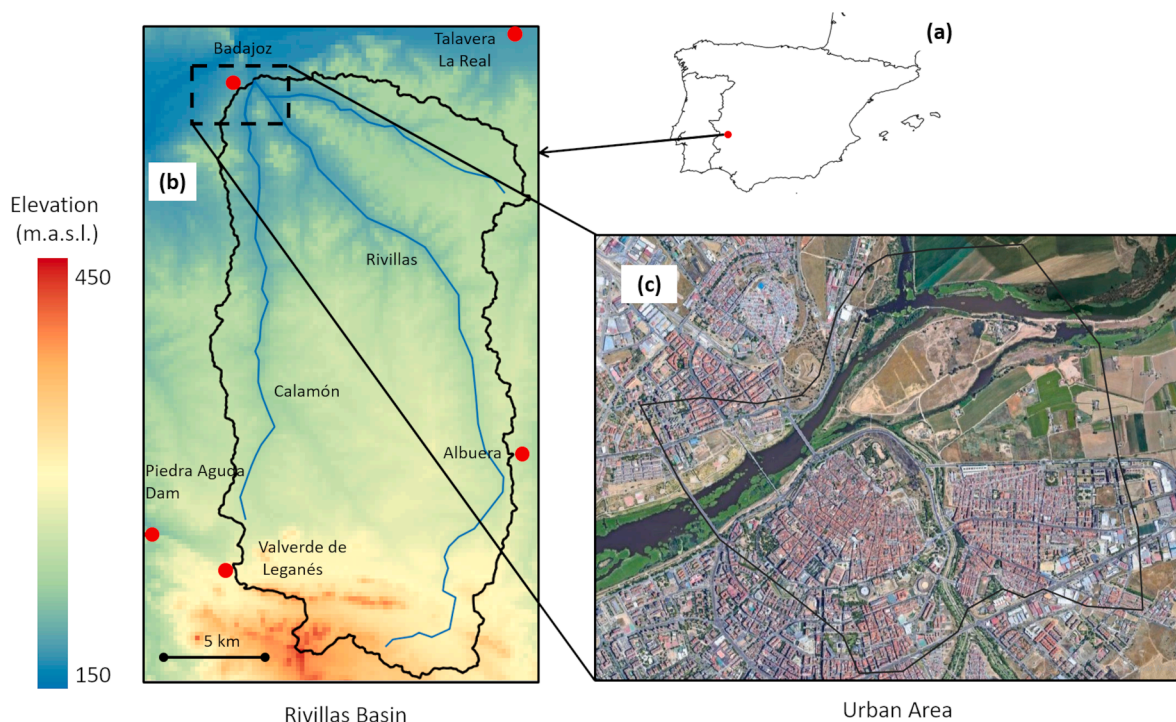
Fig. 1. Area under study: (a) location of the Rivillas river basin in the Iberian Peninsula; (b) map of elevation of the basin; (c) urban area of the Rivillas river.

far exceed previous historical peak values: 75 mm in Talavera La Real, 63.5 mm in La Albuera and 56.5 mm in Pantano de Piedraguda. The location of these rain stations is shown in Fig. 1b.

Unfortunately, only one of these stations (Talavera la Real) is equipped with a sensor that allows obtaining continuous precipitation data. The hyetograph obtained from this station shows that the precipitation event started at 15:00 of 5th November and lasted 10 h. The main stage of the event was registered between 23:00 and 24:00 of 5th November. According to testimonies, peak flows were reached in the first hours of 6th November. All these data sources and additional information allow classifying the event as a flash-flood (Brenna et al., 2020). It is also important to note that precipitation recorded during the five previous days of the flood was quite high reaching a cumulated value near 84 mm in Talavera La Real rain station. This value is a clear outlier since the mean cumulated precipitation in five days, computed using the precipitation data registered in Talavera la Real rain station from January 1980 until January 2020, is equal to 5.9 mm. This precipitation and the effect of blocked bridges located in the urban area of Badajoz amplified the height of the water maximum level and therefore increased the damages derived from the flood. According to testimonies, the bridge "Puente Nacional V" (Bridge 2 in Fig. 2) was almost totally blocked by water conduction pipes even before the event. This situation worsened during the event due the existence of heavy debris flows both in the Rivillas and Calamón rivers. These debris also blocked the bridges located upstream Bridge 2. Bridges "Cerro de Reyes", "Salvador Allende", "San Mateo", "Pardaleras" and "Puente del Obispo" (Bridges 1, 3, 4, 5 and 6 in Fig. 2) were also blocked almost from the beginning of the event. Bridges 7 to 10 (see Fig. 2) were blocked but their influence on the dramatic consequences of the event was less than the effect produced by Bridge 2 and bridges located upstream.

3. Material and methods

3.1. Precipitation dataset

The main precipitation dataset was obtained from meteorological station 4452 located in Talavera La Real base (see Fig. 1b). This station is

managed by AEMET (Agencia Estatal de Meteorología). Daily precipitation data is publicly available for the period January 1955 to January 2022 and can be freely downloaded from AEMET OpenData: (https://opendata.aemet.es/centrodedescargas/productosAEMET). Precipitation data recorded with a step-time of ten minutes was used to define the hyetograph for the simulations carried out with *Iber+*. Additional precipitation data used as complementary information in this work was obtained from the rain stations of Piedra Aguda dam (Cod.: 4484), Albuera (Cod.: CR2-42), and Badajoz (Cod.: 4478) (all represented in Fig. 1b). These stations are managed by the CHG (Confederación Hidrográfica del Guadiana).

The atypical nature of the event registered on 5–6, November 1997 is highlighted when comparing the volume of rainfall recorded during that event (119 mm) with the historical time series of daily precipitation recorded from 1876 to 2022 (Table 1).

3.2. Hydraulic model: Iber+

Iber is a numerical tool that solves the 2D depth-averaged shallow water equations using the finite volume method (Bladé et al., 2014). Recently some of the authors (García-Feal et al., 2018) have developed a new implementation of the model in C++ and CUDA (NVIDIA, 2020), namely *Iber+*. This new implementation of *Iber* improves the efficiency of the simulations by achieving a speed-up of two-orders of magnitude with the same precision by using GPU (graphical processing unit) computing HPC (high performance computing) techniques. These optimizations rise the possibility to employ the model in large spatial and temporal domains (González-Cao et al., 2020, García-Feal et al., 2020; Fernández-Nóvoa et al., 2020, Gonzalez-Cao et al., 2021) or time constrained applications (Fraga et al., 2020, González-Cao et al., 2019). Also, some applications of hybridization of *Iber+* with other Computational Fluid Dynamics (CFD) models like DualSPHysics (Domínguez et al., 2021) have been developed to analyse the behaviour of dams in high precipitation scenarios (González-Cao et al., 2018). The software package is freely available and can be downloaded from its official website (https://iberaula.es). It also includes a GUI (graphical user interface) with both pre-processing and post-processing tools. In the
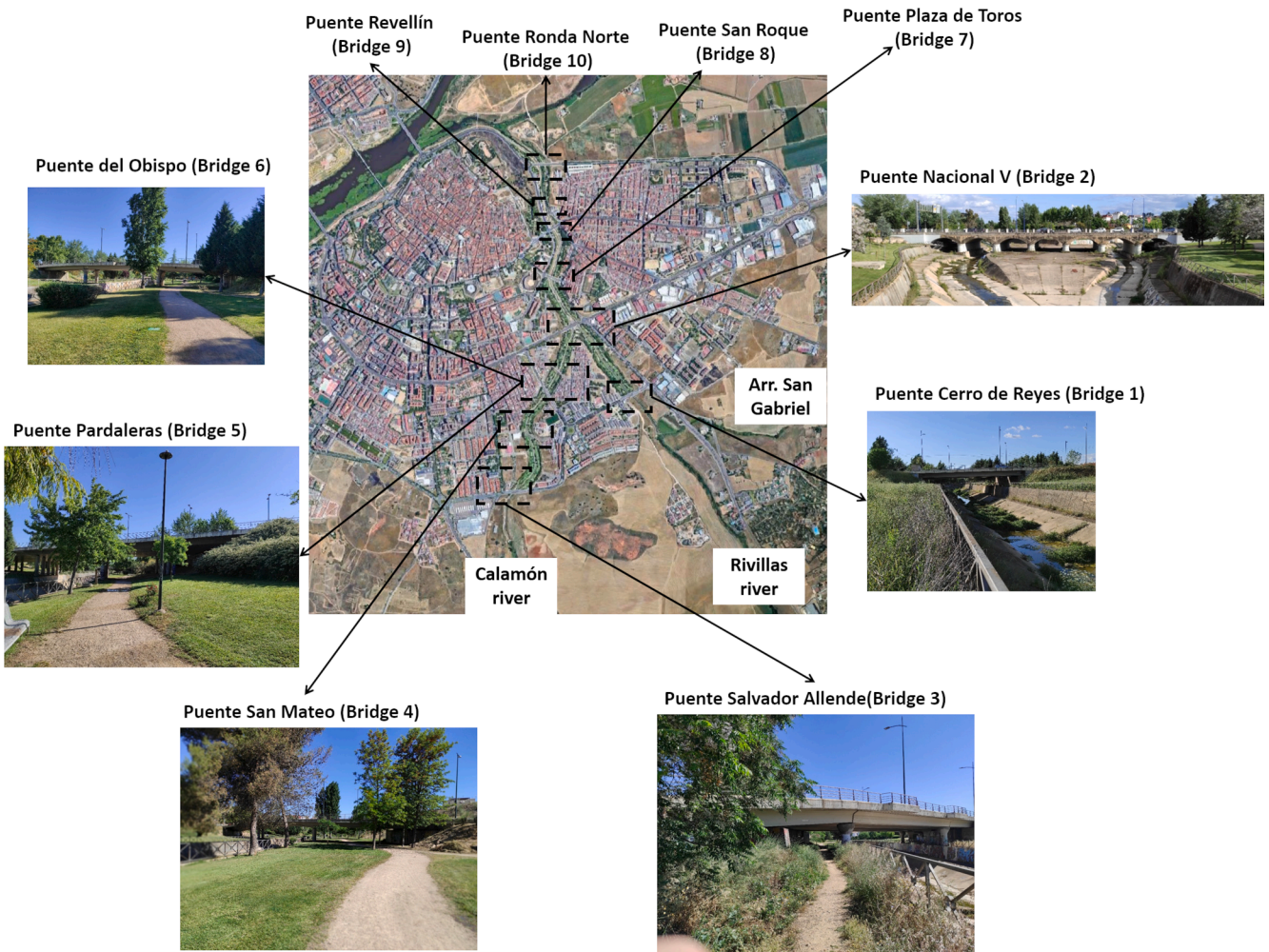
Fig. 2. Actual location of the bridges in the urban area of Badajoz.

Table 1

Peak values of daily precipitation registered in the historical time series (1876–2022) in the gauge stations located in the area of study.

Date	Daily precipitation (mm)
5/11/1997	119.1
4/11/1951	84.4
5/11/1906	83.2
16/9/1957	75.0
26/9/1928	73.7
1/2/1943	73.4
11/11/1969	70.5
3/11/1908	70.0
29/11/1910	70.0
29/11/1902	67.8

Note that the 2nd peak value was 84 mm (4/11/1951), more than 30% lower than recorded for the case under study. This approach allows identifying the event as a clear outlier in an objective way, without the high level of inaccuracy associated to other methodologies to classify extreme values as, for example, the return period (Mateo-Lázaro et al., 2016).

present study, *Iber+* was applied to the Rivillas river domain aiming to analyse the flood event registered in Badajoz (Spain) in November 1997. All the numerical simulations of Iber+ in Badajoz were performed using a GPU GeForce RTX 2080 Ti.

The domain defined in *Iber+* along with its inlet and outlet boundaries in the urban area of Badajoz is shown in Fig. 3. The inlet condition is defined as a Critical/Subcritical condition by defining the daily mean flow registered in the gage station 4030 of the CHG (Confederación Hidrográfica del Guadiana) located in Badajoz during the event and the outlet condition is defined as a Supercritical/Critical condition. The hyetograph defined corresponds to the precipitation data recorded every ten minutes at the rain station located at Talavera la Real airbase. The daily flow of Guadiana river registered in Badajoz and the precipitation registered in Talavera la Real airbase are shown in Fig. 4 (panels a and b, respectively).

The domain was discretized using a mesh of unstructured triangles whose characteristic size varies from 5 to 30 m, with a total of ~1.2 M of elements. The highest mesh size was defined to discretize the basin of the Rivillas river while the lowest values were defined to discretize urban areas of the domain in the city of Badajoz near the urban reach of the river. Medium mesh size was defined in the rest of the numerical domain. Once the numerical domain was defined and discretized, it was adapted to the topography of the area by means of a DEM (Digital Elevation Model) with a spatial resolution of 5 m that was retrieved from the web of the Centro Nacional de Información Geográfica (CNIG; http://centrodedescargas.cnig.es/CentroDescargas/index.jsp#). This DEM corresponds to current topography of the area of study. It should be stressed that some relevant modifications were carried out in the urban area in the city of Badajoz since 1997, including the widening of the river channels, upgrading works in the riverbanks of the river, and the demolition of some of the riverine buildings. However, taking into
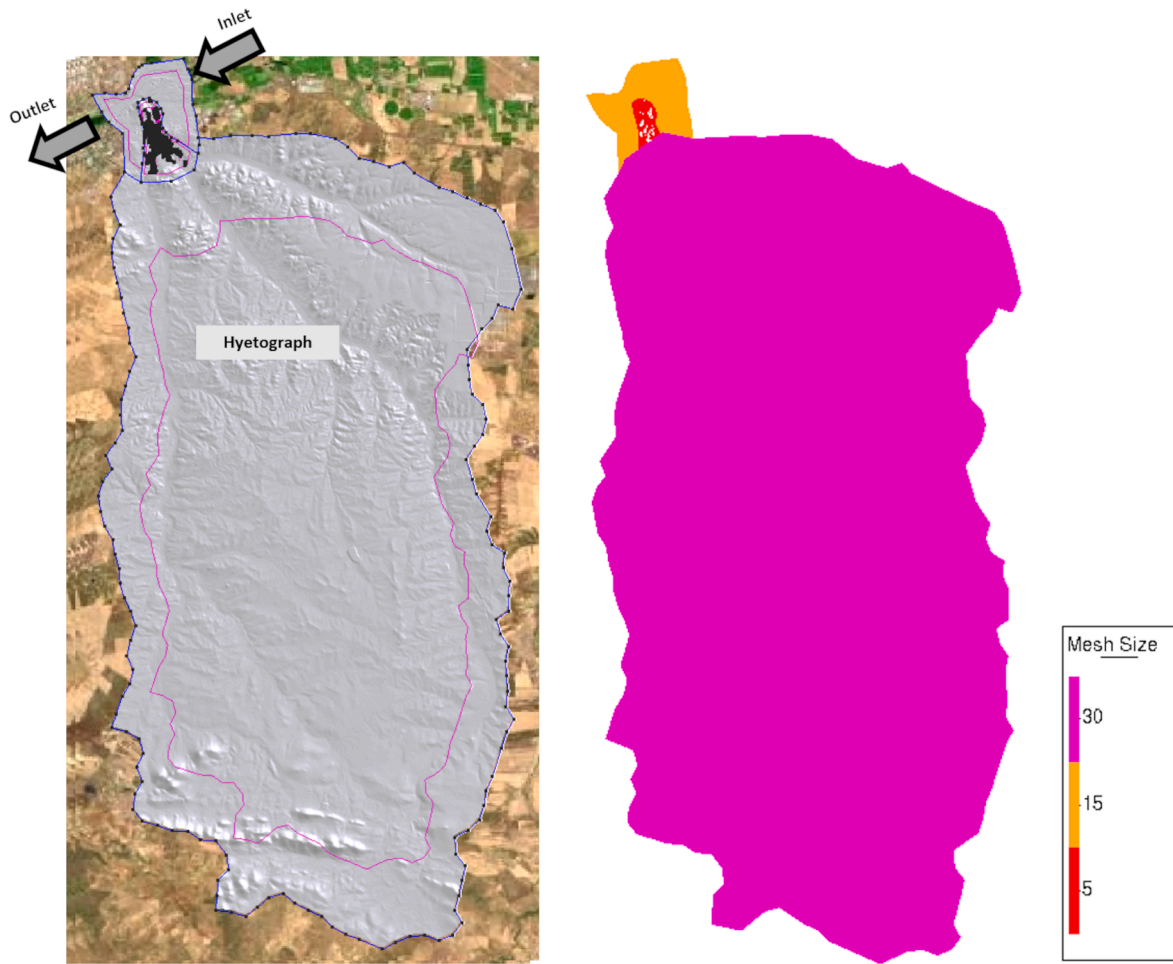
Fig. 3. Numerical domain of Rivillas river basin and topography obtained from DEM downloaded from IGN defined in *Iber+* (left) and characteristic sizes of the elements of the mesh (right).
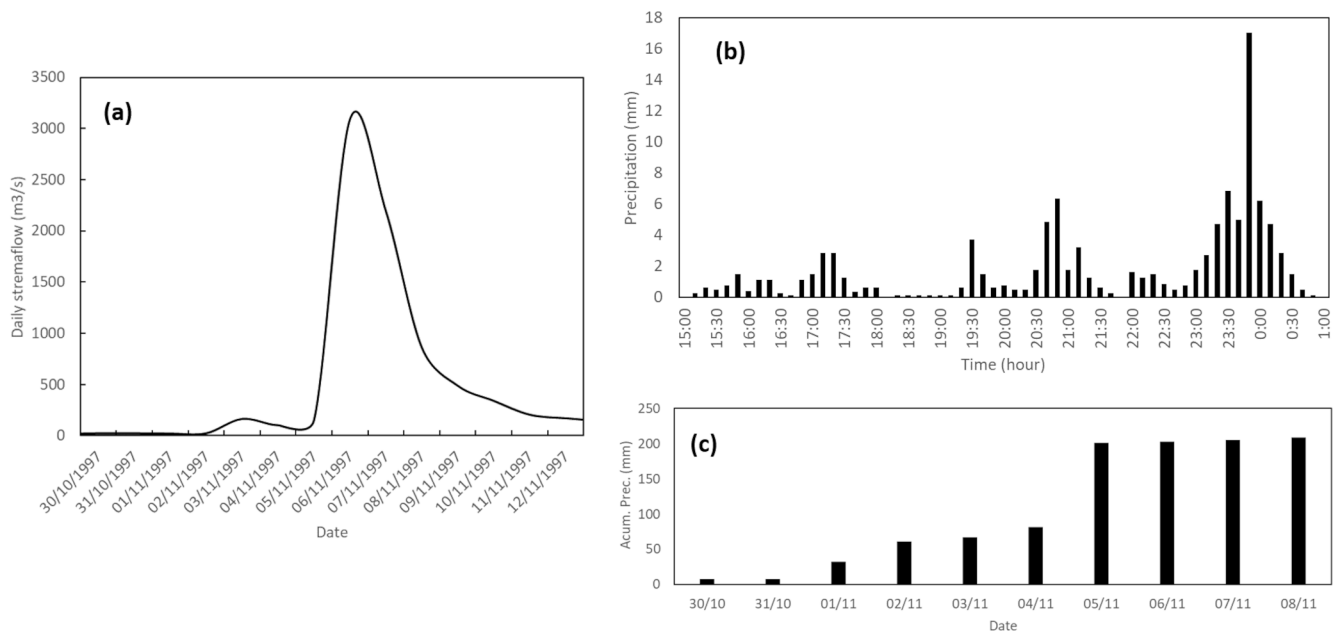

Fig. 4. Daily streamflow in Badajoz (panel a), sub-hourly precipitation registered in Talavera La Real (panel b) and accumulated precipitation registered previous days of the event (panel c).

account that these buildings were one of the main factors that increased the negative effects of the flood, we decided that they should be included in the area of study.

The 3-D shapes of the buildings were obtained by digitizing old photographs and maps of the area. Also, some footbridges were reconstructed after the flood as bridges. All these modifications were taken into account to reproduce the physical constrains that led to the event as accurately as possible. On the one hand, land uses were obtained from raster data of European Corine Land Use Land Cover data of 2000 (CLC, 2000) and, on the other hand, data of infiltration was obtained from raster file of the CN of the Iberian Peninsula computed according to the methodology proposed by Ferrer i Juliá (2003). In the present work, and taking into account that the volume of precipitation registered in the five previous days of the event is near 85 mm (see Fig. 4c), moist conditions for the CN were considered (Eq. (2)). The mean value of CN in the entire basin is equal to 85 ± 5. Fig. 5 shows the maps of land uses and CN defined in the basin of the Rivillas river.

One of the main difficulties in the numerical reproduction of historical flood events is the analysis of the uncertainty associated with the input data, that is, discharges, rainfall, DEMs, land uses and values of CNs. When it comes to more recent events, the available data is much larger than for historical events, and, therefore, the analysis of the uncertainty is an affordable task. The reader can find detailed analysis of uncertainty associated with hydrological analysis of recent events in Xu et al. (2006), Jin et al. (2010), Shen et al. (2012), Abro et al. (2020) or Nanding et al. (2021). Specifically, for the uncertainty associated with rain gauge data, Reynolds et al. (2020) show the influence of limited discharge data for flood prediction and Chen et al. (2022) show the influence of rain gauge density and distribution on Gauge-Satellite Merged Precipitation Estimates. Furthermore, the uncertainty associated with the accuracy of DEMs is often analysed for recent flood events (Pakoksung and Takagi, 2022; Xu et al., 2022). This is not the case when it comes to historical events where the amount of data is limited and therefore uncertainty analysis is beyond the scope of this type of works.

$$CN = \frac{25400}{\frac{I_a}{0.2} + 254} \quad (1)$$

$$CN_{moist} = \frac{23 \bullet CN}{10 - 0.13 \bullet CN} \quad (2)$$

According to testimonies, most of the bridges located in the urban area of the Rivillas river were partially blocked from nearly the beginning of the flood event. Therefore, in the *Iber+* simulations the bridges were considered as barriers with constant height during the entire simulation.

4. Results and discussion

4.1. Estimation of the discharge flows in Badajoz

The flows obtained with *Iber+* for Calamón and Rivillas rivers at three control points are shown in Fig. 6 with the location of these three control points represented in the left panel. Initial time of simulations corresponds to 15:00, 5th, November. Control points 1 and 2 (CP1 and CP2 in Fig. 6) correspond to flows of Calamón and Rivillas rivers, respectively, before reaching Bridge 2. Control point CPm corresponds to flow of Rivillas river near the mouth of this river. The right panel in Fig. 6 shows that the peak value of Rivillas river (obtained before Bridge 2) is higher than the peak value obtained for Calamón river (521 m³ s⁻¹ and 441 m³ s⁻¹, respectively). The maximum value of Rivillas is reached before (around 2:40 a.m) than the maximum value of the Calamón river (around 3:50 a.m) on November 6. The maximum flow value of the Rivillas river obtained at its mouth reached a value equal to 879 m³ s⁻¹ (observed at 3:00 a.m.).

4.2. Numerical analysis of the evolution of the flood event

The maximum extent of the flood obtained with *Iber+* and the corresponding maximum extent obtained from field data in the urban area of the domain are shown in Fig. 7 (left panel). The numerical results (area delimited with red lines) reproduce quite well the field data (area delimited with green lines). There are some areas (e.g. A, B and C in Fig. 7, left panel) where the numerical results overestimate the actual values of the extent. These differences can be attributed, at least partially, to the resolution of the DEM data and uncertainties associated to values of CN. The right panel of Fig. 7 shows a detailed image of the area upstream near Bridge 2 where the orange polygons refer to the buildings located within this area. It is important to notice that this area corresponds to the sector of the city most affected by the flood during this event. The blue area corresponds to the maximum flood extent situation obtained with *Iber+* confirming that it reached buildings located in both riverbanks of Calamón and Rivillas rivers. Therefore, we can
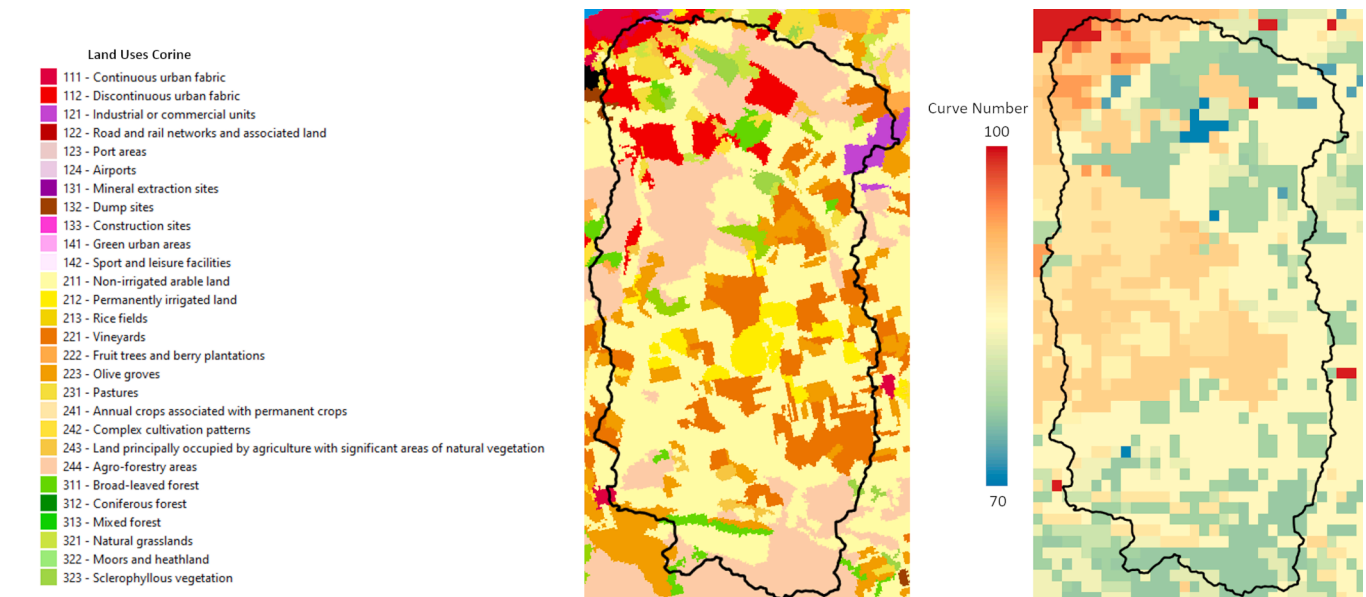

Fig. 5. Land uses obtained from Corine Land Cover (left panel) and map of curve numbers (righ panel) defined in the basin of the Rivillas river.
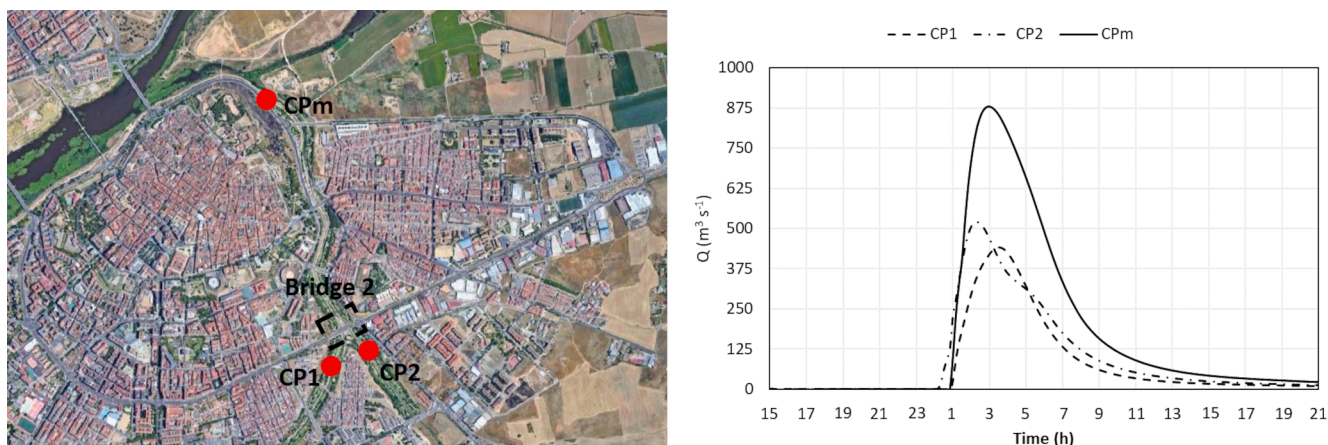
Fig. 6. Location of the control points CP1, CP2 and CPm (left panel) and discharge flow at these control points (right panel). Dashed line refers to flow obtained for Calamón river (CP1), dot-dashed line refers to flow obtained for Rivillas river before Calamón (CP2) and solid line refers to flow obtained at mouth of Rivillas river (CPm).
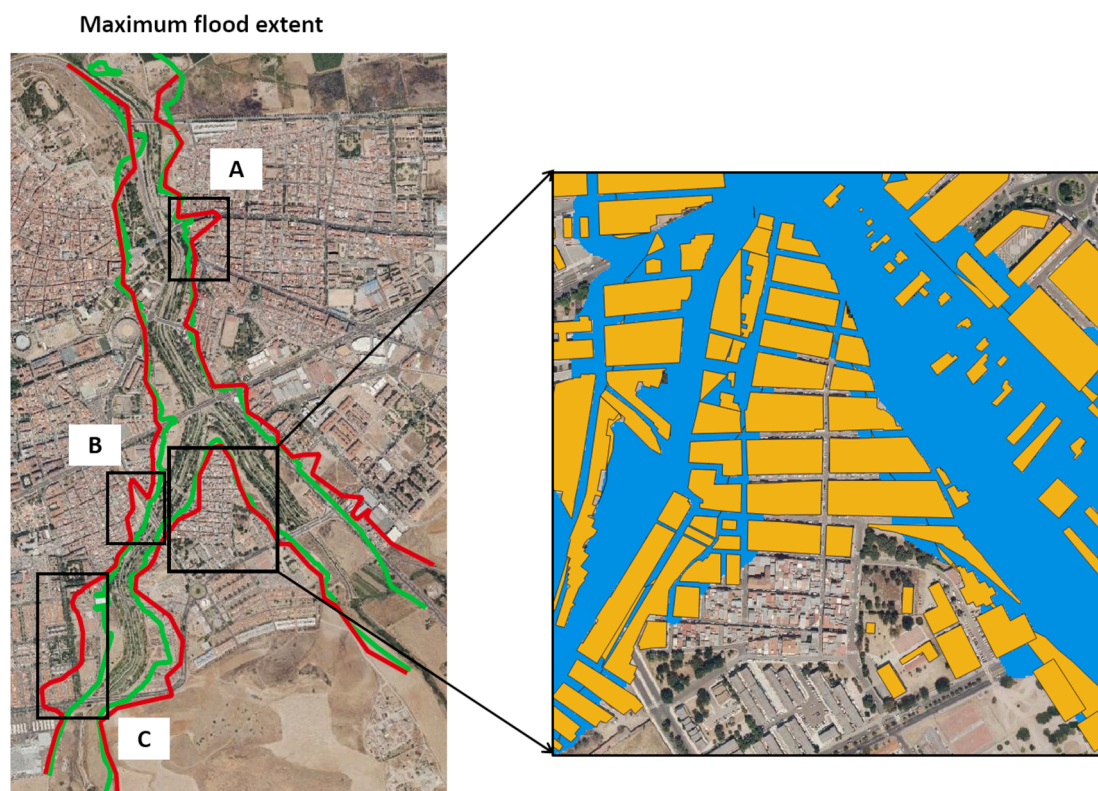
Maximum flood extent

Fig. 7. Left-panel: Maximum extent of the flood obtained in the numerical simulations (area limited by red lines) and maximum extent obtained from field data (area limited by green lines). Right panel shows a zoom over the area most affected by flood. Blue area denotes the flooded area and orange polygons represent buildings. (For interpretation of the references to colour in this figure legend, the reader is referred to the web version of this article.)

conclude that *Iber+* reproduce quite well the situation registered during the event.

However, flash flood events evolve quite rapidly and therefore require a more dynamic assessment of the areas affected, preferably at the sub-hourly temporal scale. Fig. 8 shows such evolution of the flood event water depth maps obtained with *Iber+*. From 10:20p.m. to 10:30p. m. on 5 November, flows of Rivillas and Calamón rivers arrive at urban areas of Badajoz (Fig. 8a). Flow of Rivillas river reaches the canalisation before flow of Calamón river. Near 0:45 a.m. on 6 November, flow of Rivillas impacts into Bridge 2 (Fig. 8b), while flow of Calamón overtop Bridge 4. Then, flow from Rivillas returns upstream following the Calamón riverbed (Fig. 8c). At 1:00 a.m. on 6 November, flows of Rivillas

and Calamón impact near Bridge 5. This causes the flood on the right and left riverbanks of Calamón river (Fig. 8d). The maximum extent of the flood can be observed at 2:30–3:00 a.m. on 6 November (Fig. 8e).

In addition to the evolution of the water depth maps, the evolution of water depth at five control points is represented in Fig. 9a. Control points CP1 and CP2, also depicted in Fig. 6, and CP5 and CP6 are located upstream near Bridge 2 and control point CP3 is located downstream near Bridge 2. CP1 is located in the riverbed of Calamón river while CP2 and CP3 are located in Rivillas riverbed. Control points CP4 and CP5 are located at the beginning of the canalisation of Calamón and Rivillas rivers, respectively. Fig. 9b shows that flow arrives downstream Bridge 2 at the beginning of the simulation at CP3. This flow comes from
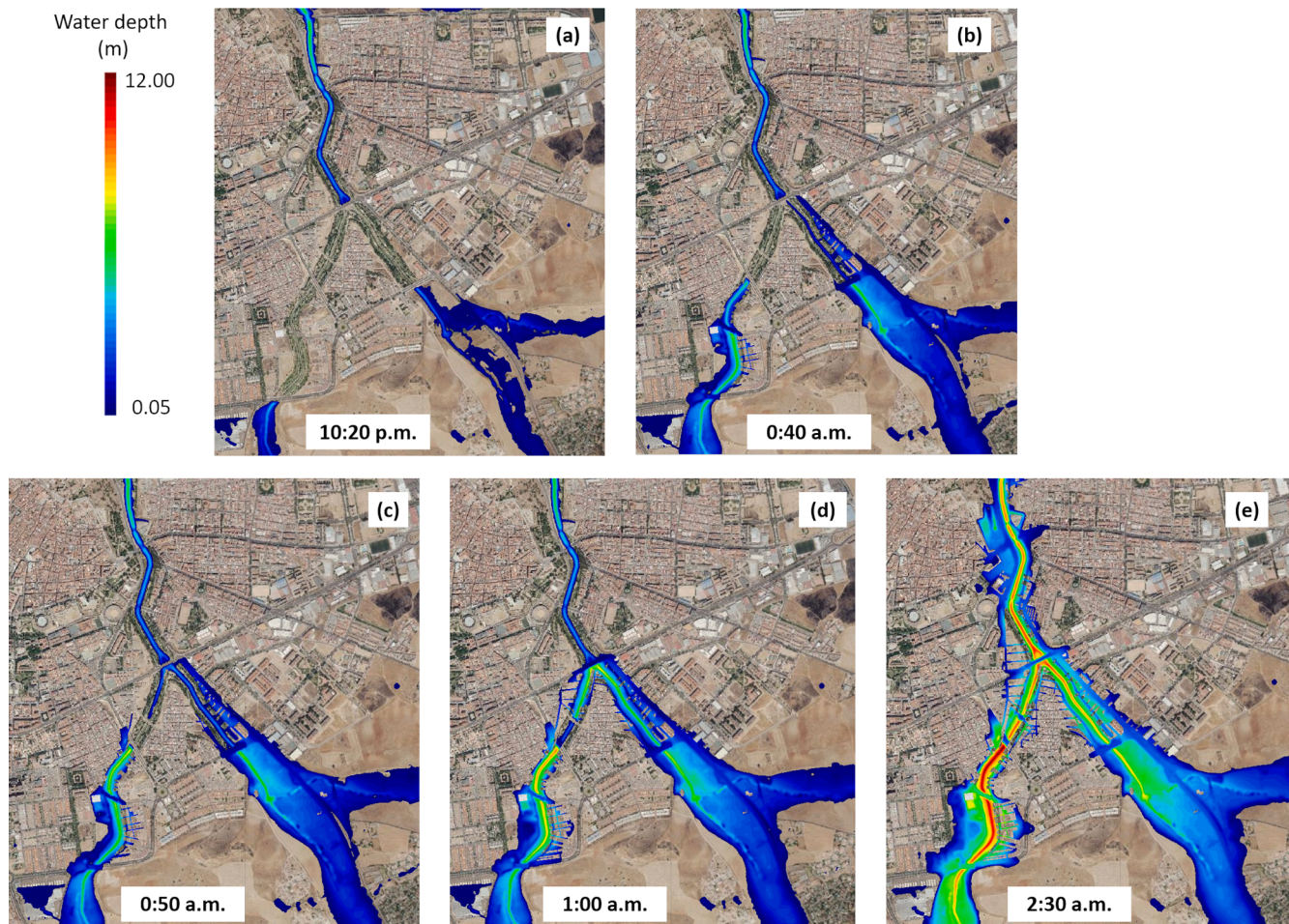
Fig. 8. Evolution of water depth maps obtained with *Iber+*. Panel (a) shows the water depth map when flood arrives to urban areas of the city; panel (b) corresponds with the instant when the flow of Calamón impacts with Bridge 2; panels (c) and (d) show to the evolution of the flood in the Calamón riverbed when the flow from Calamón and the flow from Rivillas impacts near Bridge 5; panel (e) refers to the maximum extension of the flood event (2:30 – 3:00 a.m. on 6 December).

Guadiana river. At around 1:00 a.m. on 6 November, flows from Rivillas and Calamón reach control points CP1 and CP2 respectively. From 9:00 a.m. on 6 November, water depth is higher upstream bridge 2 than downstream this bridge. This effect is due to the Bridge 2 acting as a barrier during the event. Fig. 9c confirms that flow from Calamón arrives at the starting point of the canalisation, i.e. before the flow from Rivillas river. This is because the beginning of canalisation of Calamón river is located farther away from Bridge 2 than the start of canalisation of Rivillas river.

A temporal flow chart of the numerical model evolution vs field data obtained from testimonies is shown in Fig. 10. Time evolution obtained through testimonies is quite similar to those obtained in the numerical simulations carried out with *Iber+*. Some discrepancy is observed in the timing for the maximum peak flow. Whereas timing obtained from field data is ~1:30 a.m. on 6 November, the corresponding timing from numerical simulations is situated near 3 a.m. Nevertheless, it is known that testimonies have some difficulty in defining exact timing of peak flow values during the event. This difficulty results since they can be affected by subjective perceptions as well as the lack of objective references to measure peak values. It is worth mentioning that it was night, the electric lighting stopped working and the weather conditions were adverse with rain and strong gusts of wind. Moreover, people do not usually stand at the same place during the entire event, and this can lead to misleading perceptions to define accurately the time of peak flow.

Once the numerical model has been validated to reproduce such event, a more in depth analysis was carried out. The characteristics of the implementation of *Iber+* allows an analysis of a series of

hypothetical flood scenarios considering different conditions. It can be stated, from previous analysis, that there are three main causes for the dramatic consequences of this event. First, the large amount of precipitation registered from 5:00p.m. on 5 November to 1:00 a.m. on 6 November; second, the high levels of antecedent soil moisture content due the continuous precipitation registered during the previous days of the event; third, the poor maintenance and cleaning conditions of most bridges, that quickly become partially blocked during the event. The precipitation and previous conditions of the soil are distributed over the entire basin of the river being related with meteorological conditions out of control of water management institutions. On the other hand, the conditions of the bridges only affect the urban area of the Calamón and Rivillas rivers and are directly controlled by water management institutions by means of a correct maintenance of these structures. To analyse the effect of the conditions of the bridges in the flood event, eight hypothetical scenarios with different conditions have been defined. Three different hyetographs have been defined starting from the "actual" one and reducing it a factor equal to 75%, 50% and 25%. Therefore, in this study we analyse four hyetographs: H100, H75, H50 and H25. The probability of occurrence of these three last hyetographs is much higher than the probability associated to H100. For each hyetograph two different conditions were analysed: bridges partially blocked (B-B) and free bridges (F-B). The rest of conditions associated to the event, i.e., the time distribution of the precipitation and the antecedent moisture soil content remain equal to the actual event. For each scenario we obtain the maximum hazard maps according to Cox et al. (2010) and also the time evolution of the water depth at control point CP1 (see
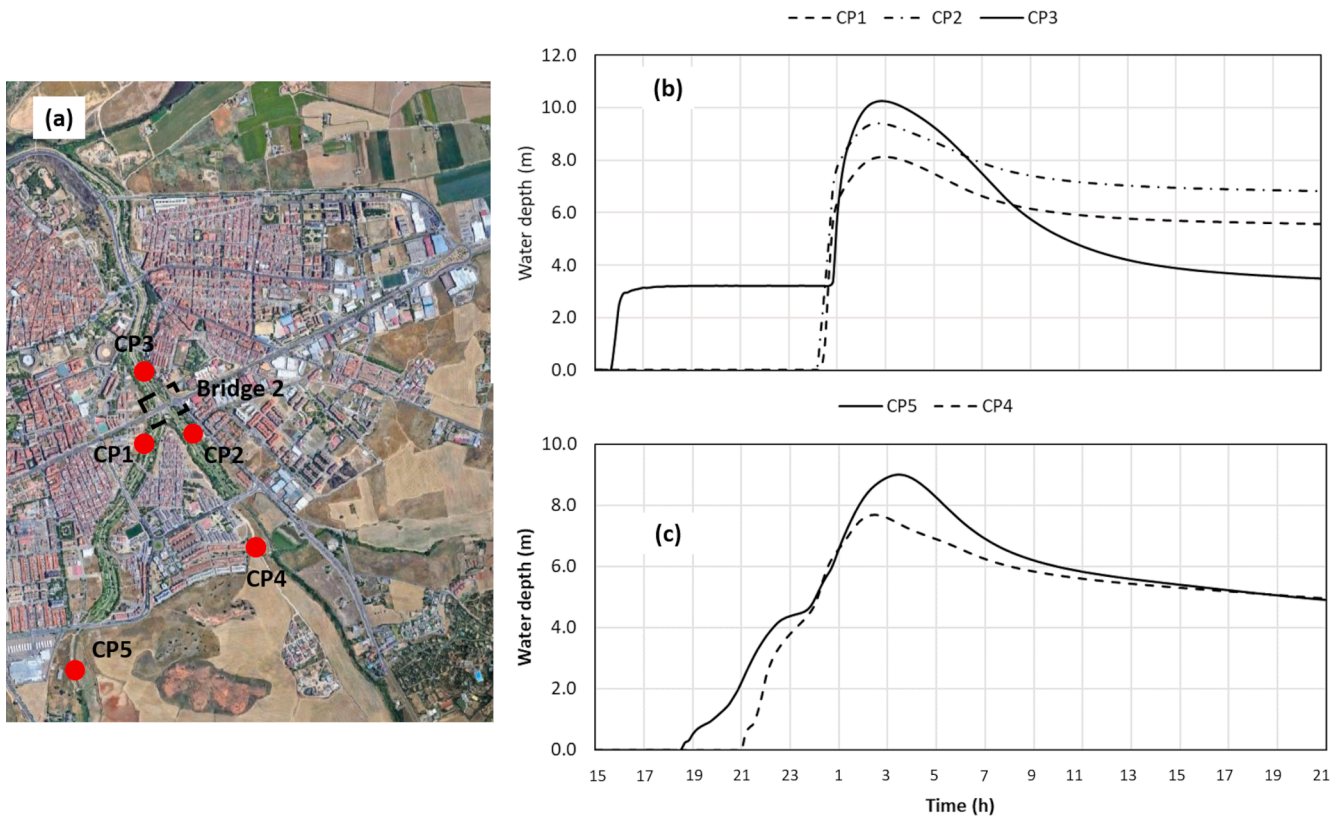
Fig. 9. Evolution of water depth obtained with *Iber+* at control points CP1, CP2 and CP3 (panel (b)) and at control points CP4 and CP5 (panel (c)). The location of these control points is shown in panel (a). Control points CP1 and CP2 are equivalent to control points depicted in upper panel of Fig. 6.
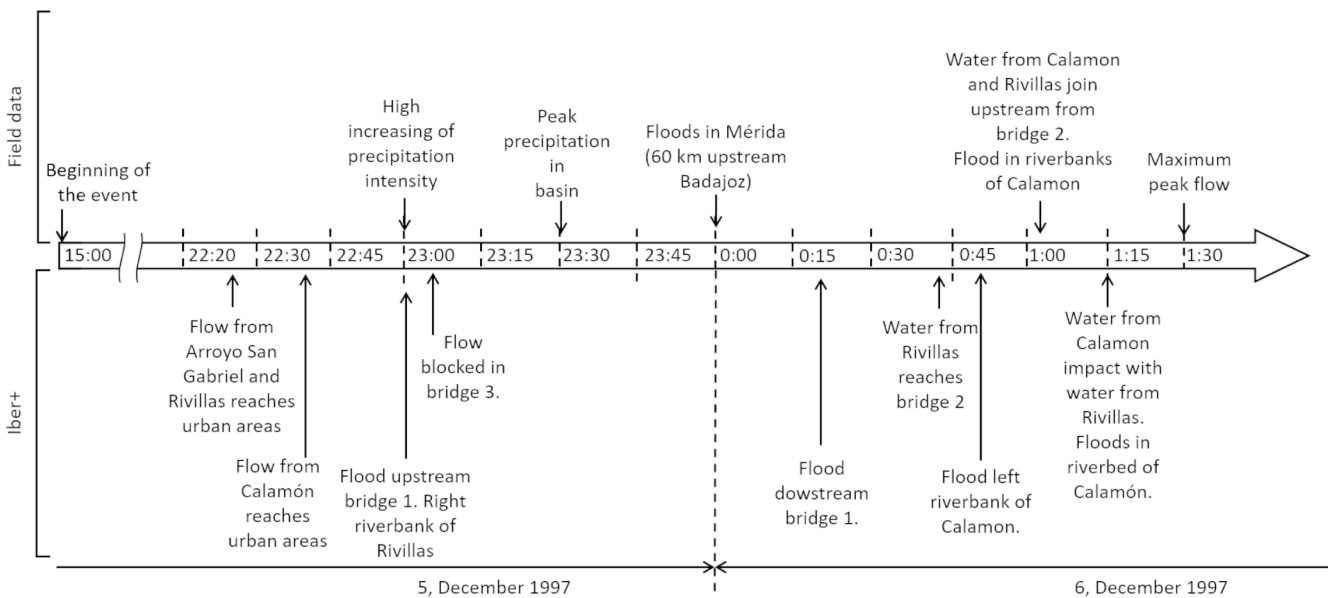

Fig. 10. Scheme of the numerical time evolution vs. field data obtained from references and testimonies.

Fig. 6). This control point is located in the area most affected during the actual flood event and, therefore, it can be considered representative to analyse the consequences of the event. The results of this analysis are shown in Fig. 11. Red areas of panels (a), (b), (c), and (d) stand for maximum hazard maps obtained with B-B condition for the four different analysed hyetographs and green areas of these panels refer to maximum hazard maps (Cox et al., 2010) obtained with F-B conditions for H100, H75, H50 and H25 hyetographs, respectively. Red and green

lines of panels (e), (f), (g) and (h) stand for time evolution of water depth with B-B and F-B, respectively, for the analysed hyetographs.

Maximum hazard maps obtained for H100 with B-B and F-B conditions (Fig. 11a) are similar to each other. Fig. 11e shows that peak values of water depth obtained for B-B and F-B are also similar: 8.1 and 7.6 m, respectively (difference ≈ 6%). This is due the high total amount of precipitation accumulated during the event. For H100, the recessing part of curve depicted in Fig. 11e obtained with B-B is lower than the
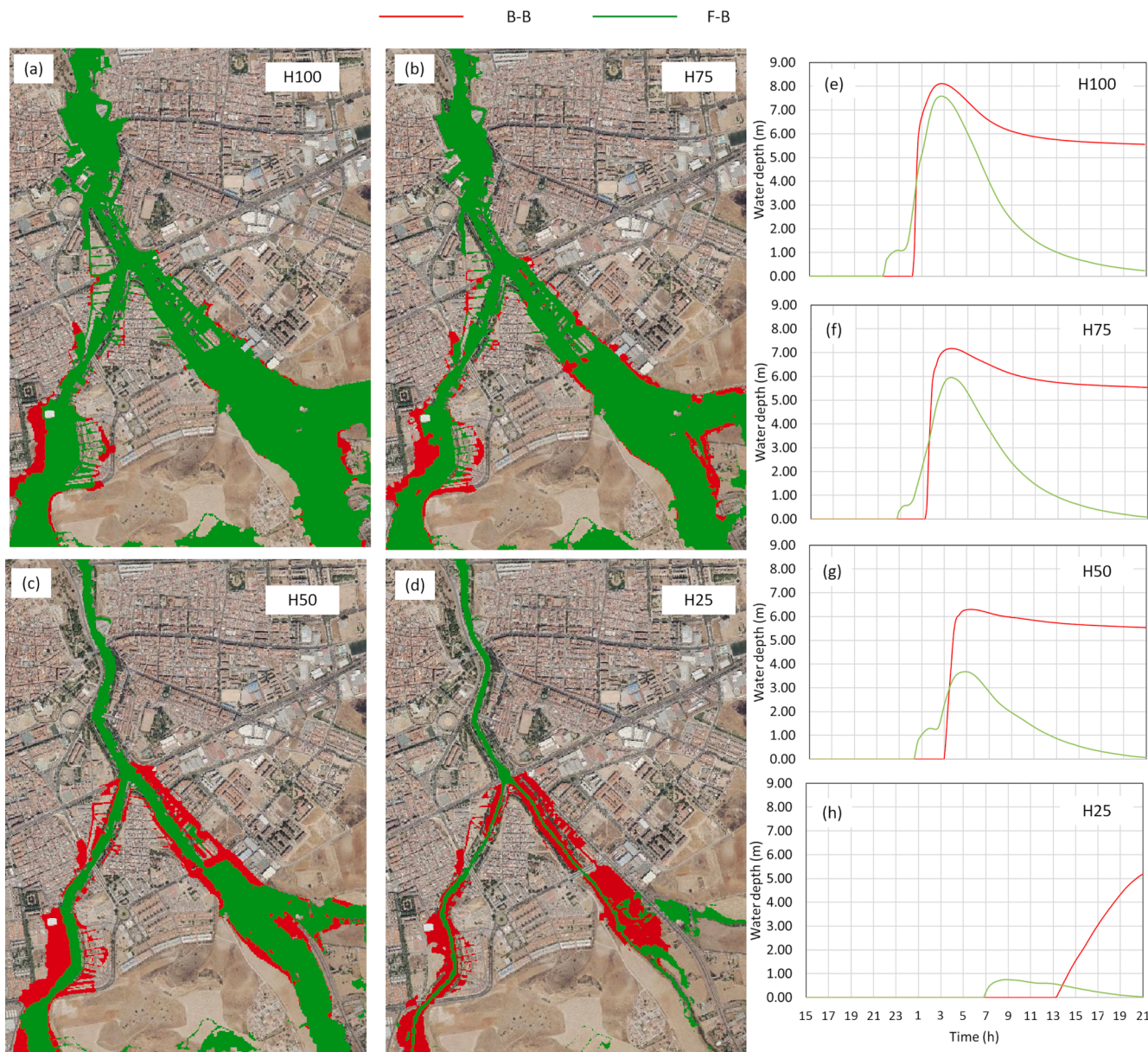
Fig. 11. Maximum hazard maps obtained with partially blocked bridges and wet conditions (B-B; red areas) and with unblocked bridges and wet conditions (F-B; green areas) for the hyetograph H100 (panel (a)), for hyetograph H75 (panel (b)), for hyetograph H50 (panel (c)) and for hyetograph H25 (panel (d)). Time evolution of water depth obtained with H100, H75, H50 and H25 are depicted in panels ((e), (f), (g) and (h)), respectively, for the analysed scenarios: B-B (red lines) and F-B (green lines). (For interpretation of the references to colour in this figure legend, the reader is referred to the web version of this article.)

recessing part of the curve obtained with F-B condition. This effect increases the negative effects of the event since it prevents the access of rescue services to affected areas. Results obtained for H75 are similar to those obtained for H100: flooded areas are similar for B-B and F-B (Fig. 11b). In this case peak values of water depth obtained with B-B and F-B are 7.1 m and 6 m, respectively. Therefore, in this case, the difference between peak values is near 15%. This indicates that the effect of blocked bridges is greater that with H100. For H50 flooded areas downstream Bridge 2 obtained for B-B and F-B (Fig. 11c) are similar but the difference between the flooded areas upstream Bridge 2 are evident. Fig. 11g shows that peak value of water depth for B-B is much higher (6.3 m) than peak value obtained with F-B condition (3.7 m). The difference between these values (2.6 m) is greater than the difference between peak values obtained with the same conditions but for H100 and H75 (0.6 m and 1.2 m, respectively) and represents a drop of almost 45%. This stresses that for this case (H50) the effect of blocked bridges

increases its influence in the flooded areas versus the amount of water registered during the precipitation event. This effect is even more obvious for H25, as in this case flooded areas obtained with B-B (Fig. 11d) conditions are much higher than those obtained with F-B. Peak value of water depth obtained with B-B is near 5 m while peak value obtained with F-B conditions is less than 1 m (corresponding to 80% less). Finally, the values of wet areas obtained with the four analysed hyetographs and the B-B and F-B conditions in the urban area of the Rivillas river are depicted in Fig. 12. For both conditions wet areas increase as the amount of precipitation increases. Wet areas obtained with B-B conditions are 31 ha, 50 ha, 65 ha and 73 ha for each hyetograph while for corresponding F-B conditions wet areas are 12 ha, 30 ha, 56 ha and 67 ha. The difference of wet areas obtained with B-B and F-B conditions decreases as peak values of hyetographs increases. For H25 and H50 the difference is equal to 19 ha and 20 ha, respectively, for H75 is equal to 9 ha and for H100 is equal to 6 ha. This means that the effect
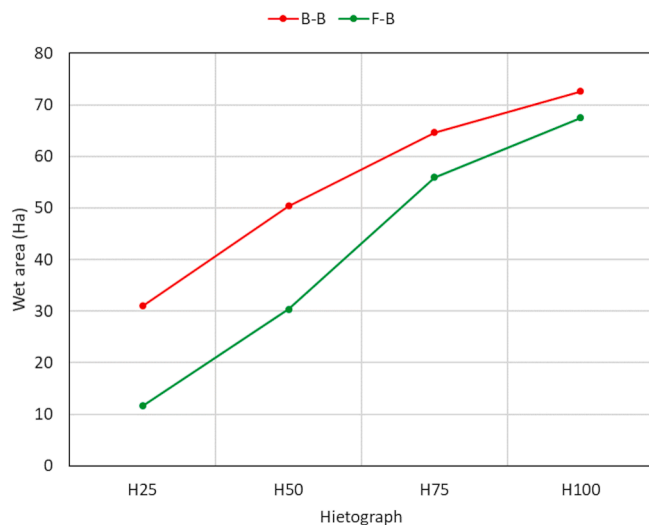
Fig. 12. Wet areas obtained with the analysed hyetographs and B-B (red line) and F-B (green line conditions. (For interpretation of the references to colour in this figure legend, the reader is referred to the web version of this article.)

of the blocked bridges decreases as the amount of precipitation increases. This is in accordance with the results of water depth.

5. Conclusions

In this work, the numerical simulation of the flood event registered in Badajoz on 5th and 6th in November 1997 was carried out by means of the *Iber+*. This event corresponds to one of the most catastrophic urban flash floods registered in the Iberian Peninsula in the 20th century. The unprecedented level of this event is summed up by the amount of precipitation registered during the event, the number of fatalities (21), and the economic losses.

The numerical simulations carried out with *Iber+* allows undertaking the coupled analysis the urban area and the rest of the basin of the Rivillas river. The urban area of the river is characterized by the canalization of the main stream of the Rivillas river as well as of the main tributary of this river, i.e, the Calamón river. In this urban area, the existence of several bridges and buildings had a crucial impact in the evolution and the consequences of the urban flood, especially for medium intensity hydrographs.

The numerical results obtained with *Iber+* reproduce quite well the event registered in 1997 both the extension and the temporal evolution of the flood compared with field data. Also, peak values of water depths are in agreement with data provided by testimonies.

One of the conclusions of this work is that with a similar deficient maintenance, the same temporal evolution and maximum flooded areas recorded during the past event would be reached today. Obviously, the demolition of the houses located near the river bed would minimize the negative effects under a similar event. According to the analysis, there were three main factors that increased the negative effects of the event: (1) the amount of precipitation registered from 5:00p.m. on 5 November to 1:00 a.m. on 6 November; (2), the high levels of antecedent soil moisture content; (3), the poor maintenance condition of bridges, partially blocked during the event.

A series of hypothetical scenarios were considered to assess the effect of precipitation and the maintenance conditions of the bridges during the event. Four hyetographs (H100, H75, H50 and H25) and two maintenance conditions (partially blocked or free bridges) were analysed. The results show that a significant part of the area can be flooded even with low intensity hyetographs, especially when the span of the bridge is blocked. The flooded area is much smaller when the bridge is not blocked.

In summary, the work has highlighted *Iber+*'s ability to reproduce extreme flash flood events in urban areas. Moreover, the model allowed designing hypothetical scenarios that can help to a better maintenance of hydraulic structures. This can constitute a powerful tool within the present framework of climate change.

CRediT authorship contribution statement

José González-Cao: Conceptualization, Formal analysis, Investigation, Methodology, Resources, Visualization, Writing – original draft. **Diego Fernández-Nóvoa:** Conceptualization, Formal analysis, Investigation, Methodology. **Orlando García-Feal:** Formal analysis, Investigation, Methodology. **Jose R. Figueira:** Conceptualization, Formal analysis, Investigation, Methodology, Resources. **José M. Vaquero:** Conceptualization, Resources, Supervision, Writing – review & editing. **Ricardo M. Trigo:** Conceptualization, Resources, Supervision, Writing – review & editing. **Moncho Gómez-Gesteira:** Conceptualization, Formal analysis, Investigation, Supervision, Writing – review & editing.

Declaration of Competing Interest

The authors declare that they have no known competing financial interests or personal relationships that could have appeared to influence the work reported in this paper.

Acknowledgements

References

Abro, M.I., Zhu, D., Ali Khaskheli, M., Elahi, E., Aleem ul Hassan Ramay, M., 2020. Statistical and qualitative evaluation of multi-sources for hydrological suitability inflood-prone areas of Pakistan. J. Hydrol. 588, 125117.

Aranda, J.Á., Beneyto, C., Sánchez-Juny, M., Bladé, E., 2021. Efficient design of road drainage systems. Water (Switzerland) 13 (12), 1661. https://doi.org/10.3390/w13121661.

Bárdossy, A., Anwar, F., Seidel, J., 2020. Hydrological modelling in data sparse environment: inverse modelling of a historical flood event. Water (Switzerland) 12 (11), 3242. https://doi.org/10.3390/w12113242.

Bartholmes, J., Todini, E., 2005. Coupling meteorological and hydrological models for flood forecasting. Hydrol. Earth Syst. Sci. 9 (4), 333–346. https://doi.org/10.5194/hess-9-333-2005.

Beniston, M., 2009. Trends in joint quantiles of temperature and precipitation in Europe since 1901 and projected for 2100. Geophys. Res. Lett. 36 (7).

Benito, G., Machado, M. J. y Pérez González, A., 1996. Climate change and flood sensivity in Spain. En: Brarndson, J., Brown, A. G. y Gregory, K. L. (Eds). global continental Changes: the context of palaeohydrology. Geological Society Special Publication n° 115, 85-98. Londres.

Benito, G., Castillo, O., Ballesteros-Cánovas, J.A., MacHado, M., Barriendos, M., 2021. Enhanced flood hazard assessment beyond decadal climate cycles based on centennial historical data (Duero basin, Spain). Hydrol. Earth Syst. Sci. 25 (12), 6107–6132. https://doi.org/10.5194/hess-25-6107-2021.

Bergström, S., 1992. The HBV Model: Its Structure and Applications. SMHI Reports Hydrology; SMHI, Norrköping, Sweden.

Bermúdez, M., Farfán, J.F., Willems, P., Cea, L., 2021. Assessing the effects of climate change on compound flooding in coastal river areas. Water Res 57 (10).

Bladé, E., Cea, L., Corestein, G., Escolano, E., Puertas, J., Vázquez-Cendón, E., Dolz, J., Coll, A., 2014. Iber: herramienta de simulación numérica del flujo en ríos. Revista Internacional de Métodos Numéricos para Cálculo y Diseño en Ingeniería 30 (1), 1–10.

Bonasia, R., Ceragene, M., 2021. Hydraulic numerical simulations of la Sabana river floodplain, Mexico, as a tool for a flood terrain response analysis. Water (Switzerland) 13 (24), 3516. https://doi.org/10.3390/w13243516.

Brenna, A., Surian, N., Ghinassi, M., Marchi, L., 2020. Sediment–water flows in mountain streams: recognition and classification 580 based on field evidence. Geomorphology 371. https://doi.org/10.1016/j.geomorph.2020.107413.

Buzzi, A., Tartaglione, N., Malguzzi, P., 1998. Numerical simulations of the 1994 piedmont flood: role of orography and moist processes. Mon. Weather Rev. 126 (9), 2369–2383. https://doi.org/10.1175/1520-0493(1998)126<2369:NSOTPF>2.0.CO;2.

Cedex.,, 1998. Estudio sobre las inundaciones ocurridas el día 6 de noviembre de 1997 en Badajoz, Valverde de Leganés y Mérida. Informe II (Badajoz), Madrid.

Chao, L., Zhang, K., Yang, Z.-L., Wang, J., Lin, P., Liang, J., Li, Z., Gu, Z., 2021. Improving flood simulation capability of the WRF-Hydro-RAPID model using a multi-source precipitation merging method. J. Hydrol. 592, 125814.

Chen, Y., Huang, J., Song, X., Wen, H., Song, H., 2022. Evaluation of the impacts of rain gauge density and distribution on gauge-satellite merged precipitation estimates. IEEE Trans. Geosci. Remote Sens. 60, 1–18.

CLC. © European Union, Copernicus Land Monitoring Service 2000, European Environment Agency (EEA).

Cox, R.J., Shand, T.D., Blacka, M.J., 2010. Australian Rainfall and Runoff revision project 10: appropriate safety criteria for people. Water Res. 978, 085825–89454.

Domínguez, J.M., Fourtakas, G., Altomare, C., Canelas, R.B., Tafuni, A., García-Feal, O., Martínez-Estévez, I., Mokos, A., Vacondio, R., Crespo, A.J.C., Rogers, B.D., Stansby, P.K., Gómez-Gesteira, M., 2021. DualSPHysics: from fluid dynamics to multiphysics problems. Comput. Particle Mech. https://doi.org/10.1007/s40571-021-00404-2.

E.D. European Directive2007/60/C.

EFAS, European Flood Awareness System, 2021. https://www.efas.eu/en/news/widespread-european-flooding-july-2021. Last acces: November, 2021.

Elleder, L., Krejčí, J., Šírová, J., 2020a. The 1714 flash flood in the Bohemian-Moravian Highlands – Reconstructing a Catastrophe. Quat. Int. 538, 14–28. https://doi.org/10.1016/j.quaint.2019.02.002.

Elleder, L., Krejčí, J., Racko, S., Daňhelka, J., Šírová, J., Kašpárek, L., 2020b. Reliability check of flash-flood in Central Bohemia on May 25, 1872. Global and Planetary Change 187, 103094. https://doi.org/10.1016/j.gloplacha.2019.103094.

Eulenstein, J., Kellerer-Pirklbauer, A., 2020. The central European flood of 1572 and its local scale effects as revealed by a damage inventory. Hydrol. Sci. J. 65 (6), 884–897. https://doi.org/10.1080/02626667.2020.1716980.

Fernández-Nóvoa, D., García-Feal, O., González-Cao, J., de Gonzalo, C., Rodríguez-Suárez, J.A., del Portal, C.R., Gómez-Gesteira, M., 2020. MIDAS: a new integrated flood early warning system for the Miño River. Water (Switzerland) 12 (9), 3420. https://doi.org/10.3390/W12092319.

Ferre i Juliá, M. Análisis de nuevas fuentes de datos para la estimación del parámetro número de curva: perfiles de suelos y teledetección, 2003. Editor. :CEDEX. ISBN: 84-7790-389-1.

Font, I., 1988. Historia del clima en España. Cambios climáticos y sus causas. Instituto Nacional de Meteorología. 297p. Madrid.

Fraga, I., Cea, L., Puertas, J., 2020. MERLIN: a flood hazard forecasting system for coastal river reaches. Nat. Hazards 100 (1171–1193), 7.

García-Alén, G., García-Fonte, O., Cea, L., Pena, L., Puertas, J., 2021. Modelling weirs in two-dimensional shallow water models. Water (Switzerland) 13 (16), 2152. https://doi.org/10.3390/w13162152.

García-Feal, O., González-Cao, J., Gómez-Gesteira, M., Cea, L., Domínguez, J.M., Formella, A., 2018. An accelerated tool for flood modelling based on Iber. Water 10, 1459.

García-Feal, O., Cea, L., González-Cao, J., Domínguez, J.M., Gómez-Gesteira, M., 2020. IberWQ: a GPU accelerated tool for 2D water quality Modeling in Rivers and Estuaries. Water 12, 413.

González, A., 1995. Badajoz cara al Guadiana: Puerta de Palmas y el Puente Viejo (1460–1994). Caja Rural de Extremadura, Badajoz.

Gonzalez-Cao, J., Fernández-Nóvoa, D., García-Feal, O., Figueira, J.R., Vaquero, J.M., Trigo, R.M., Gómez-Gesteira, M., 2021. Numerical reconstruction of historical extreme floods: The Guadiana event of 1876. J. Hydrol., 126292 https://doi.org/10.1016/j.jhydrol.2021.126292.

González-Cao, J., García-Feal, O., Domínguez, J.M., Crespo, A.J.C., Gómez-Gesteira, M., 2018. Analysis of the hydrological safety of dams combining two numerical tools: Iber and DualSPHysics. J. Hydrodyn. 30 (1), 87–94. https://doi.org/10.1007/s42241-018-0009-6.

González-Cao, J., García-Feal, O., Fernández-Nóvoa, D., Domínguez-Alonso, J.M., Gómez-Gesteira, M., 2019. Towards an automatic early warning system of flood hazards based on precipitation forecast: the case of the Miño River (NW Spain). Nat. Hazards Earth Syst. 19.

González-Cao, J., García-Feal, O., Fernández-Nóvoa, D., Domínguez-Alonso, J.M., Gómez-Gesteira, M., 2020. *Iber+:* a new code to analyse dam-break floods. In: In book: Advances in Natural Hazards and Hydrological Risks: Meeting the Challenge, pp. 165–169. https://doi.org/10.1007/978-3-030-34397-2_32.

Groisman, P.Y., Knight, R.W., Easterling, D.R., Karl, T.R., Hegerl, G.C., Razuvaev, V.N., 2005. Trends in intense precipitation in the climate record. J. Climate 18 (9), 1326–1350. https://doi.org/10.1175/JCLI3339.1.

Hermoso, A., Homar, V., Amengual, A., 2021. The sequence of heavy precipitation and flash flooding of 12 and 13 September 2019 in eastern Spain. Part i: mesoscale

diagnostic and sensitivity analysis of precipitation. J. Hydrometeorol. 22 (5), 1117–1138. https://doi.org/10.1175/JHM-D-20-0182.1.

IPCC, 2021. In: Masson-Delmotte, V., Zhai, P., Pirani, A., Connors, S.L., Péan, C., Berger, S., Caud, N., Chen, Y., Goldfarb, L., Gomis, M.I., Huang, M., Leitzell, K., Lonnoy, E., Matthews, J.B.R., Maycock, T.K., Waterfield, T., Yelekçi, O., Yu, R., Zhou, B. (Eds.), Climate Change 2021: The Physical Science Basis. Contribution of Working Group I to the Sixth Assessment Report of the Intergovernmental Panel on Climate Change. Cambridge University Press.

Jin, X., Xu, C.-Y., Zhang, Q., Singh, V.P., 2010. Parameter and modeling uncertainty simulated by GLUE and a formal Bayesian method for a conceptual hydrological model. J. Hydrol. 383 (3–4), 147–155. https://doi.org/10.1016/j.jhydrol.2009.12.028.

Laguarda, M., 1962. Las inundaciones de Valencia de 1957. Memoria oficial de la Delegación Permanente del Gobierno. 251 pp, Talleres Gráficos Miguel Laguardia.

Mateo-Lázaro, J., Sánchez Navarro, J.T., García Gil, A., Edo Romero, V., 2016. Flood Frequency Analysis (FFA) in Spanish catchments. J. Hydrol. 538, 598–608. https://doi.org/10.1016/j.jhydrol.2016.04.058.

Mateo-Lázaro, J., Castillo-Mateo, J., García-Gil, A., Sánchez-Navarro, J.A., Fuertes-Rodríguez, V., Edo-Romero, V., 2020. Comparative hydrodynamic analysis by using two-dimensional models and application to a new bridge. Water (Switzerland) 12 (4), 997. https://doi.org/10.3390/W12040997.

Máyer Suárez, P., 2002. Lluvias e inundaciones en la Ciudad de Las Palmas (1699-1999). ISBN: 978-84-95286-99-4.

Morss, R.E., Wilhelmi, O.V., Meehl, G.A., Dilling, L., 2011. Improving societal outcomes of extreme weather in a changing climate: an integrated perspective. Annu. Rev. Environ. Resour. 36, 1–25. https://doi.org/10.1146/annurev-environ-060809-100145.

Nanding, N., Rico-Ramirez, M.A., Han, D., Wu, H., Dai, Q., Zhang, J., 2021. Uncertainty assessment of radar-raingauge merged rainfall estimates in river discharge simulations. J. Hydrol. 603, 127093 https://doi.org/10.1016/j.jhydrol.2021.127093.

NVIDIA Corporation CUDA C++ Programming Guide Available online: https://docs.nvidia.com/cuda/pdf/CUDA_C_Programming_Guide.pdf (accessed on Aug. 27, 2020).

Ortega, J.A., 2007. Paleocrecidas, Avenidas recientes e Hidroclimatología en la Cuenca Media y Baja del río Guadiana. Departamento de Geodinámica, Facultad de Ciencias Geológicas, Universidad Complutense de Madrid, Spain (PhD thesis).

Pakoksung, K., Takagi, M., 2022. Effect of DEM sources on distributed hydrological model to results of runoff and inundation area. Model. Earth Syst. Environ. 7 (3), 1891–1905. https://doi.org/10.1007/s40808-020-00914-7.

Pfister, C., Brázdil, R., Glaser, R., Barriendos, M., Camuffo, D., Deutsch, M., Dobrovolny, P., Enzi, S., Guidoboni, E., Kotyza, O., Militzer, S., Racz, L., Rodrigo, F.S., 1999. Documentary evidence on climate in the sixteenth-century Europe. Special issue: climatic variability in sixteenth-century Europe and its social dimensions. Clim. Change 43 (1), 55–110.

Reynolds, J.E., Halldin, S., Seibert, J., Xu, C.Y., Grabs, T., 2020. Flood prediction using parameters calibrated on limited discharge data and uncertain rainfall scenarios. Hydrol. Sci. J. 65 (9), 1512–1524. https://doi.org/10.1080/02626667.2020.1747619.

Ruman, S., Tichavský, R., Šilhán, K., Grillakis, M.G., 2021. Palaeoflood discharge estimation using dendrogeomorphic methods, rainfall-runoff and hydraulic modelling—a case study from southern Crete. Nat. Hazards 105 (2), 1721–1742. https://doi.org/10.1007/s11069-020-04373-2.

Shen, Z.Y., Chen, L., Chen, T., 2012. Analysis of parameter uncertainty in hydrological and sediment modeling using GLUE method: a case study of SWAT model applied to Three Gorges Reservoir Region, China. Hydrol. Earth Syst. Sci. 16 (1), 121–132. https://doi.org/10.5194/hess-16-121-2012.

Trigo, R.M., Varino, F., Ramos, A.M., Valente, M.A., Zêzere, J.L., Vaquero, J.M., Gouveia, C.M., Russo, A., 2014. The record precipitation and flood event in Iberia in December 1876: description and synoptic analysis. Front. Earth Sci. 2 (April), 3 https://doi.org/10.3389/feart.2014.00003.

Trigo, R.M., Ramos, C., Pereira, S.S., Ramos, A.M., Zêzere, J.L., Liberato, M.L.R., 2016. The deadliest storm of the 20th century striking Portugal: flood impacts and atmospheric circulation. J. Hydrol. 541, 597–610. https://doi.org/10.1016/j.jhydrol.2015.10.036.

Vennari, C., Parise, M., Santangelo, N., Santo, A., 2016. A database on flash flood events in Campania, southern Italy, with an evaluation of their spatial and temporal distribution. Nat. Hazards Earth Syst. Sci. 16 (12), 2485–2500. https://doi.org/10.5194/nhess-16-2485-2016.

Xu, C.-Y., Tunemar, L., Chen, Y.D., Singh, V.P., 2006. Evaluation of seasonal and spatial variations of lumped water balance model sensitivity to precipitation data errors. J. Hydrol. 324 (1–4), 80–93. https://doi.org/10.1016/j.jhydrol.2005.09.019.

Xu, K., Fang, J., Fang, Y., Sun, Q., Wu, C., Liu, M., 2022. The importance of digital elevation model selection in flood simulation and a proposed method to reduce DEM errors: a case study in Shanghai. Int. J. Disaster Risk Sci. 12 (6), 890–902. https://doi.org/10.1007/s13753-021-00377-z.

Zamora-Cabanillas, J.F., 1999. Consideraciones sobre la riada sucedida en la ciudad de Badajoz en Noviembre de 1997. Monografía: La Ciencia a las puertas del Tercer Milenio (I), Catedra Nova.

Zêzere, J.L., Pereira, S.S., Santos, P.P., 2020. A century and half of hydrogeomorphological disasters in mainland Portugal. Adv. Sci. Technol. Innov. 3–6. https://doi.org/10.1007/978-3-030-34397-2_1.